AD-A105 930 HOUSTON UNIV TEX DEPT OF MECHANICAL ENGINEERING F/G 20/1
ACOUSTO-OPTICAL TOMOGRAPHY INVESTIGATION OF ULTRASONIC FIELD.(U)
1979 B D COOK N00014-79-C-0469
UNCLASSIFIED NL

(11)

(9) Final Report,

to the

(15) Office of Naval Research
Contract No: N00014-79-C-0469

1 JUN 1981 (11) 1979

(6) ACOUSTO-OPTICAL TOMOGRAPHY
INVESTIGATION OF ULTRASONIC FIELD

(12) 17 submitted by

(10) Bill D. Cook
Department of Mechanical Engineering
Cullen College of Engineering
University of Houston Central Campus
Houston, Texas 77004

401241

The proposed research was to apply the principles of computer aid tomography to acousto-optic data for the purpose of investigating sound radiation and scattering. The principal investigator had previously developed the theory and logic but lacked the facilities, namely for computer acquisition, mass storage, display of the large amounts of information involved. The objective of this contract was to allow the principal investigator and colleagues at the Navy Research Laboratory, Washington, DC to implement the necessary hardware and computer algorithms during the semester of 1979. The Physical Acoustics Branch of the Naval Research Laboratory had both the acousto-optic facilities and the on-line computer system. Upon submission of the proposal, the principal investigator sent to the scientific personnel at NRL, the requirements for the manipulation of the acoustic radiating system. The personnel there designed a manipulator and ordered the required parts to build the device.

The plan of action was for the principal investigator to become familar with the computer system while the manipulator was being built. The parts required for the manipulator were not received during the summer of 1979.

Consequently, the Principal Investigator devoted himself to theoretical and computational problems of interest of the Physical Acoustics Branch. The computer

experiments underway at NRL pertaining to acousto-optics and radiation of sound fields.

ACOUSTO-OPTICS

In as much as tomography may be considered as the inversion of a scattering process, the Principal Investigator developed an algorithm to calculate the direct process of scattering of light by ultrasound. The algorithm is novel in that, one needs only to specify the nature of radiating acoustic transducer and many of the observed acousto-optic phenomena can be predicted and graphically displayed. Attachment A and B are publications resulting from this activity.

FOCUSED ULTRASONIC FIELDS

An ongoing activity on the Physical Acoustic Branch of NRL was experimental exploration of focused ultrasonic fields. The Principal Investigator had recently supervised a PhD student on the theory of such fields. A joint experimental and computational effort was made to validate the theory. Attachment C is a publication which shows the success of the activity.

ACOUSTO-OPTIC TOMOGRAPHY

The contract was extended to May 1980 to allow the Principal Investigator to publish the material and

continue his theoretical investigation at the University of Houston. During this period he developed a new theory of data acquisition for acousto-optic tomography, trained two undergraduates and submitted a new proposal to the Office of Naval Research in addition to publishing. The new proposal was funded by ONR and the two students and the Principal Investigator returned to NRL for the Summer of 1980 to continue the research.

A Numerical Procedure for Calculating the Integrated Acoustooptic Effect

BILL D. COOK, SENIOR MEMBER, IEEE, EDUARDO CAVANAGH, AND HENRY D. DARDY, MEMBER, IEEE

Abstract—The integrated optical effect of light passing through an ultrasonic field can be numerically calculated from the velocity distribution assigned to a planar transducer. The theory is developed for linear acoustics, nonabsorbing media, and normal incidence of light. As a consequence of the application of the Fourier projection slice theorem, an algorithm based on digital Fourier transforms calculates the integrated optical effect without integration. Demonstrations of the influence of transducer geometry are shown for the integrated optical effect and schlieren patterns based on this effect.

INTRODUCTION

THE OPTICAL methods for estimating field quantities, such as pressure, of ultrasonic fields required a model of the sound field. Often these were simplistic (collimated plane waves) but very useful. In reality the light usually passes through the near-field region of the ultrasonic transducer. The multitude of schlieren photographs in the literature give testimony to the complexity of the effect of the near field. For example, Fig. 1 shows a schlieren image, published by Osterhammel [1] in 1941, of the near field of a square transducer. The intricate pattern was explained by Osterhammel as interference of planes waves from the face of transducer and circular waves from the edge; this theory does not permit quantitative calculations and is not extendable to other geometries.

Schlieren patterns such as is shown in Fig. 1 can be computed provided the field parameters of the integrated optical effect are known. At low ultrasonic frequencies, the interaction of sound and light can be described by one parameter, the so-called Raman-Nath parameter v [2]. For a three-dimensional pressure field $p(x, y, z)\, e^{i\omega t}$, with the light traversing in the y direction as shown in Fig. 2, the integrated optical effect is defined as

$$v(x, z) = \frac{2\pi\kappa}{\lambda} \int p(x, y, z)\, dy. \tag{1}$$

Here λ is the optical wavelength and κ is the piezooptic coefficient. The integrated optical effect is thus a two-dimensional phasor field $v(x, z)$. In this paper a computation procedure is presented for calculating $v(x, z)$ when the motion of the transducer is specified. The procedure is straightforward and eased by utilization of the standard one-dimensional Fourier transform which yields the field $v(x, z)$ at a given z as a one-step process.

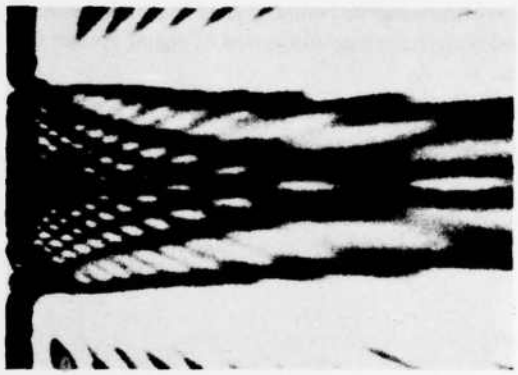

Fig. 1. Schlieren photograph of near field of a square transducer with ratio of width to acoustical wavelength of 14.37, from Osterhammel [1].

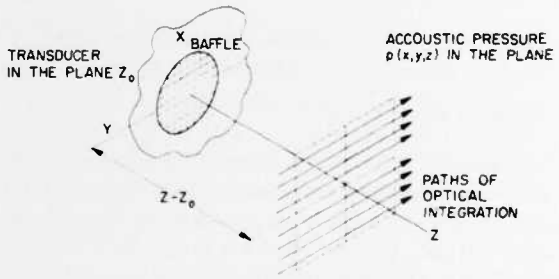

Fig. 2. Diagram showing geometry.

Analytic solutions and numerical procedures have been attempted on the problem previously. Ingenito and Cook [3] have given an exact formulation for piston-like motions of the transducers with on-axis values given in approximation for a circular, rectangular, and square piston on its diagonal. Maloney, Meltz, and Gravel [4] have treated the square transducer with the Fresnel approximation. Their experimental measurements in solids agreed with theory for both axial and transverse profiles. Crandal [5] also made computations and measurements with emphasis on phase measurements for sound velocity measurements. Haran, Cook, and Stewart [6] have used the theoretical results for comparing optical calibration of a circular transducer with a radiation pressure technique. Riebold *et al.* [7], [8] have also made careful mea-

Manuscript received December 5, 1979; revised March 1, 1980. This work was supported in part by the Office of Naval Research in conjunction with the Physical Acoustics Branch, Navy Research Laboratory, Washington, DC.

B. D. Cook and E. Cavanagh are with the Cullen College of Engineering, University of Houston, Central Campus, Houston, TX 77004.

H. D. Dardy is with the Naval Research Laboratory, Washington, DC 20375.

0018-9537/80/0400-0202$00.75

surements on the axis values to compare with the theory of Igenito and Cook [3]. Berlinghieri and Cook [9] have also calculated the v-field for a circular piston to test an inversion algorithm to estimate the pressure $p(x, y, z)$ from measured values of $v(x, z)$.

The procedure presented here allows calculations throughout the near field including the adjacent region to the transducer where the pressure field and integrated optical effect can vary significantly with a small change of position. The only limitation in calculating the complete field appear to be those connected with the normal utilization of digital Fourier transforms.

Theory

The procedure that is to be developed is based on the application of the Fourier projection slice theorem in conjunction with the Fourier technique of solving the scalar wave equations. Briefly the Fourier projection slice theorem states that the one-dimensional transform

$$W(k_x) = \int_{-\infty}^{\infty} w(x) \exp(ik_x x)\, dx \tag{2}$$

of the projection $w(x)$, defined as

$$w(x) = \int_{-\infty}^{\infty} f(x, y)\, dy \tag{3}$$

is equivalent to the two-dimensional Fourier transform $F(k_x, k_y)$ with $k_y = 0$. In other words it states

$$W(k_x) = F(k_x, k_y = 0). \tag{4}$$

Consequently, a knowledge of a slice of Fourier domain yields $w(x)$ upon the inverse transform. The theorem is to be applied to (1) which is now recognized as the form of a projection integral. Thus the scheme is to find the Fourier slice $P(k_x, k_y = 0; z)$ corresponding to the local value $p(x, y, z)$ of the pressure produced by a given normal particle velocity $u(x, y; z = 0)\, e^{i\omega t}$ of the transducer; and then numerically compute the inverse transform.

A common method of approaching scalar radiation problems is by resolving the field parameter, i.e., pressure, velocity potential, etc., into a system of plane waves with two-dimensional Fourier transforms. For example, let

$$P(k_x, k_y; z) = \iint p(x, y, z) \exp[-i(k_x x + k_y y)]\, dx\, dy \tag{5}$$

and

$$p(x, y, z) = (\tfrac{1}{2}\pi)^2 \iint P(k_x, k_y; z) \cdot \exp[i(k_x x + k_y y)]\, dk_x\, dk_y \tag{6}$$

be a typical transform pair. Here $p(x, y, z)$ is a phasor, as previously defined, that satisfies the Helmholtz equation

$$\nabla^2 p + k^2 p = 0 \tag{7}$$

as in the case of linear nonabsorbing acoustic waves. Substituting (6) into (7), one can obtain

$$\frac{d^2 P}{dz^2} + (k^2 - k_x^2 - k_y^2) P = 0. \tag{8}$$

A solution of (8) is

$$P(k_x, k_y; z) = P(k_x, k_y; z_0) \exp[-ik_z (z - z_0)] \tag{9}$$

where $k_z = (k^2 - k_x^2 - k_y^2)^{1/2}$. Thus, this approach permits calculation of the field in the plane z from a knowledge of the field in the plane z_0. The quantity $P(k_x, k_y; z)$ can be interpreted as the phasor description of plane waves with wave vector (k_x, k_y, k_z). It is noted that k_z can be real, which means that the wave propagates, or imaginary which infers an evanescent wave.

Our intermediate objective is to find $P(k_x, k_y; z)$ from the velocity distribution of the transducer. We started with one component of the force equation

$$\frac{\partial p}{\partial z} = -\rho \frac{\partial u_z}{\partial t} \tag{10a}$$

$$= -i\omega u_z \qquad \text{(for harmonic waves)} \tag{10b}$$

where the z axis is in the direction normal to the transducer surface and ρ is the density of the medium. Substituting (9) for the pressure and a similar expression for the particle velocity into (10) one can find

$$P(k_x, k_y; z) = (k/k_z)\, \rho c\, U_z(k_x, k_y; z) \tag{11}$$

where c is the velocity of sound. Equation (11) is the plane wave relationship between pressure and particle velocity; the term (k/k_z) in the secant of the angle between the direction of propagation of the plane and the z direction when k_z is real.

At this stage of the development, we know how to evaluate $v(x, z)$ from $P(k_x, 0; z)$ and to calculate $P(k_x, 0; z)$ at any plane z from $P(k_x, 0; z_0)$ which are related to a Fourier domain description of the z component of the particle velocity $u_z(k_x, 0; z_0)$. To obtain $u_z(k_x, 0; z_0)$ from the given particle velocity $u_z(x, y, z_0)$, we again apply the Fourier projection slice theorem. We take the projection of $u_z(x, y, z_0)$ to be

$$\bar{U}_z(x, z_0) = \int u_z(x, y, z_0)\, dy \tag{12}$$

where the y direction is chosen to be the direction of light propagation. The one-dimensional transform of $\bar{U}_z(x, z_0)$ is $U_z(k_x, 0; z_0)$ our desired result.

Thus the procedure for calculating the field $v(x, z)$ is as follows.

1) For a given direction of light propagation with respect to transducer geometry, calculate the projection of velocity by (12).
2) Numerically compute the one-dimensional Fourier transform to find $U_z(k_x, 0; z_0)$.
3) Divide by k_z and the other appropriate constants to obtain $P(k_x, 0; z_0)$ as specified by (11).
4) Calculate $P(k_x, 0; z)$ at desired plane z using (9).

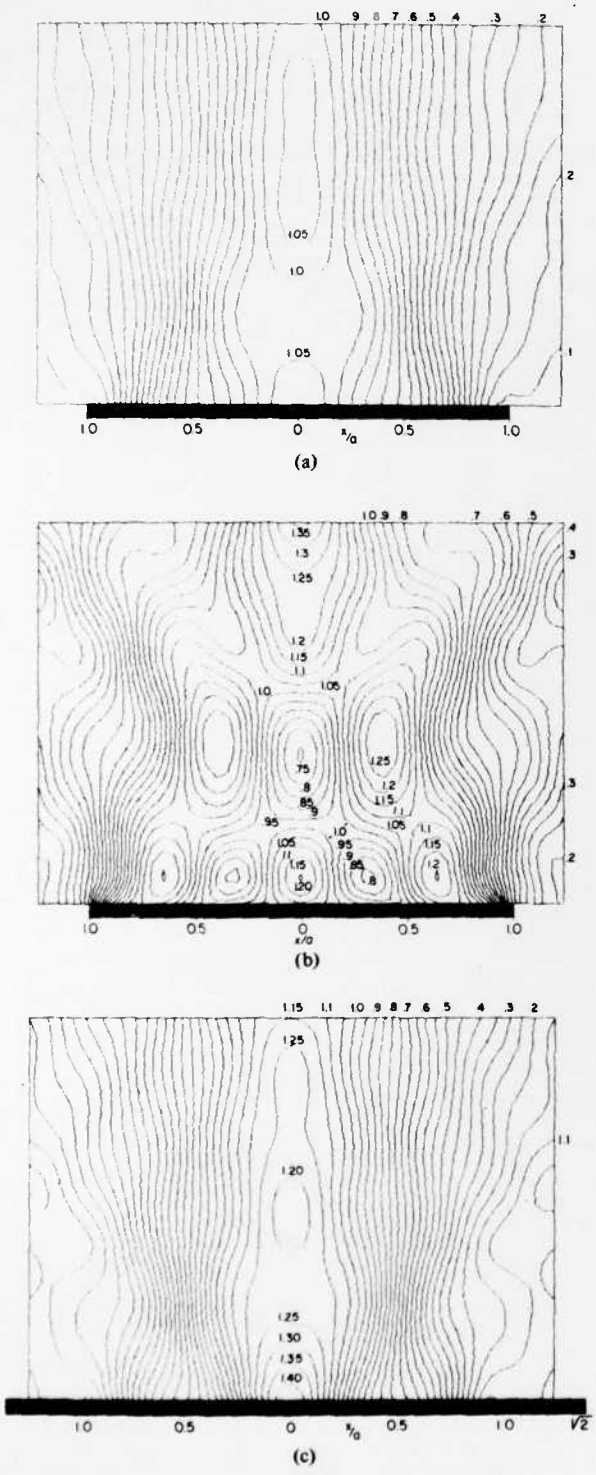

Fig. 3. Computed integrated optical effect (normalized for $ka = 10$. (a) Circular transducer. (b) Rectangular. (c) Square on diagonal.

5) Compute the inverse one-dimensional transform to evaluate $v(x, z)$.

To calculate at alternate distance z from the transducer, repeat steps 4) and 5).

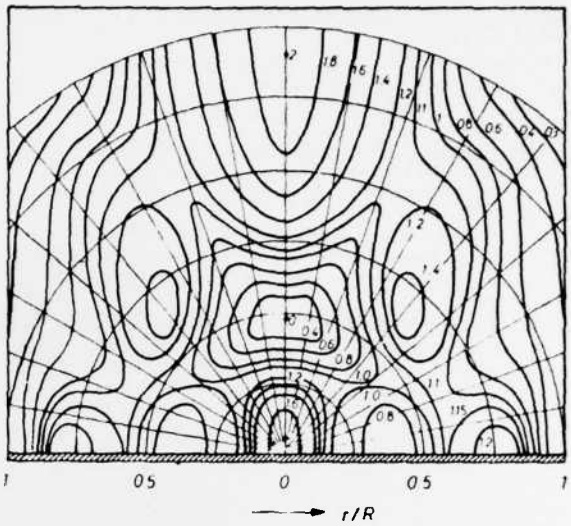

Fig. 4. Computed local variation of pressure for a circular piston with $ka = 10$, from Meyer and Newman [11]. (Courtesy of Academic Press).

Results

Using the procedure described above we have calculated the integrated optical effect for a circular, rectangular, and square transducer on its diagonal with $ka = 10$. The dimension a is the radius of a circular transducer, half the length of a side of the square transducer and half the length of the rectangular transducer perpendicular to the direction of light propagation. The field variations of $v(x, z)$ for these configurations are shown in Fig. 3. Assuming the rectangular transducer is square the normalization $v_0 = 4\pi\kappa a/\lambda$ has been applied for all of these configurations.

The field variations are observed to be considerably different in three configurations. The rectangular transducer has the largest variations, the circular next and the square on the diagonal being the most uniform. The results agree with the observations by Cook and Ingenito [10] and the calculations along the axis of Ingenito and Cook [3].

The variation in the integrated optical effect are not as large as the variations in the local value of pressure. Fig. 4 shows the variation in pressure generated by a circular transducer of $ka = 10$ for comparison with Fig. 3(a).

Having the field values of $v(x, z)$ allows one to calculate photographs of schlieren patterns from first principles. To demonstrate how the transducer geometry and sound level affects the schlieren, we present a series of computed schlieren patterns. The spatial filter of the schlieren was chosen to pass only the zeroth diffraction order. The patterns were calculated by assigning each point in relative intensity

$$I_0 = J_0^2(v(x, z)) \tag{13}$$

where $J_0(v)$ is the zeroth order Bessel function of the first kind. A logarithmic response of the film was assumed and a gray scale assigned. Figs. 5, 6, and 7 correspond to the fields of Fig. 3(a), 3(b), and 3(c) at various sound levels. In each case the value of v listed is the maximum value found anywhere in the field. At low levels, there is a correspondence be-

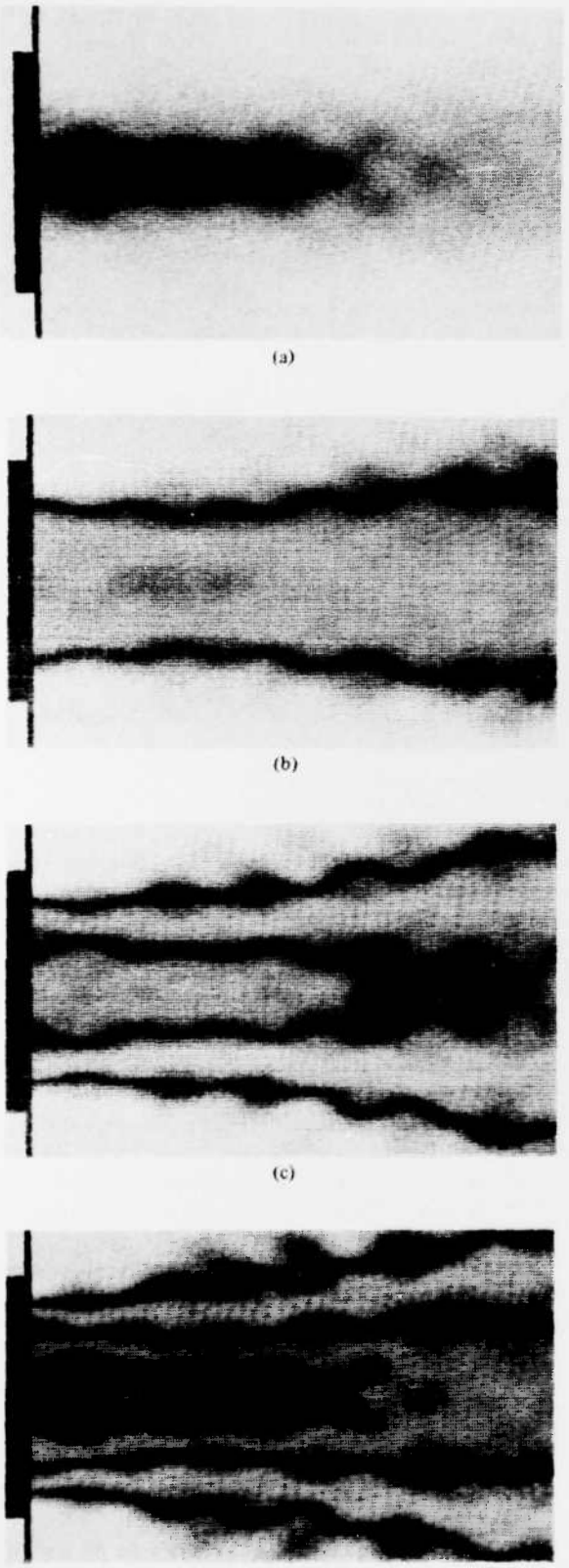

Fig. 5. Computed bright field schlieren for circular transducer at various sound levels. (a) $v = 2.5$. (b) $v = 5.0$. (c) $v = 7.5$. (d) $v = 10.0$.

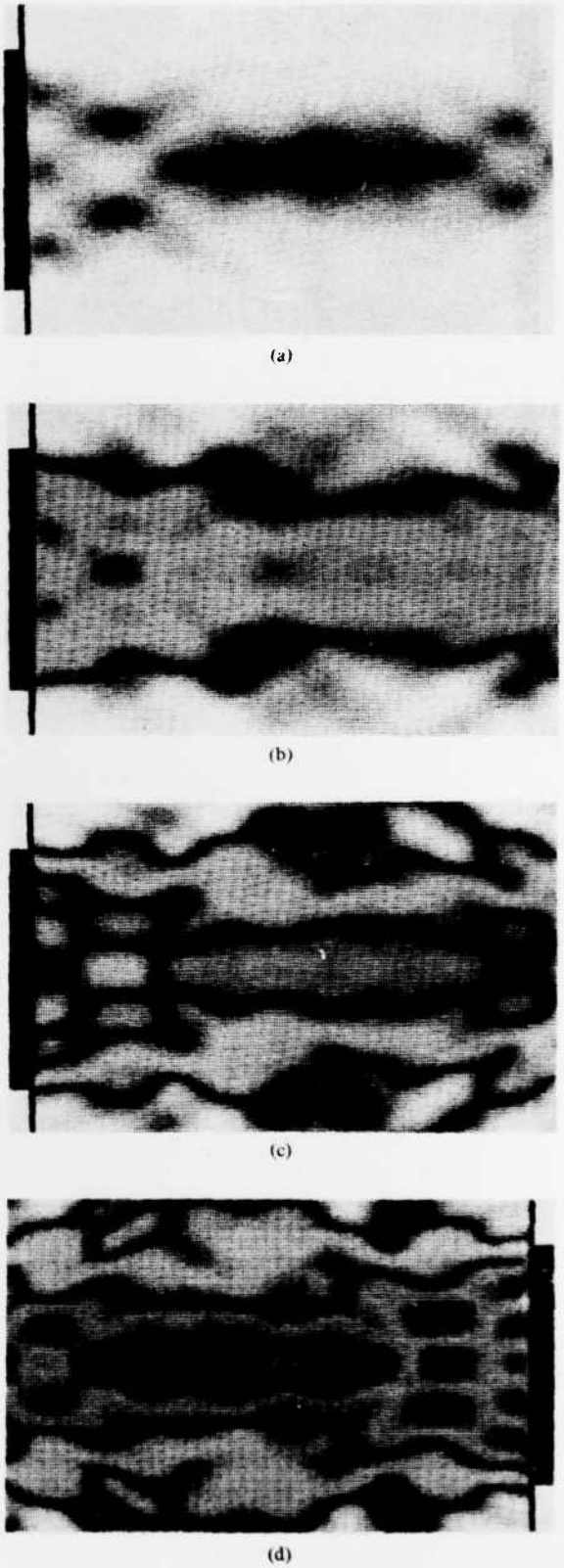

Fig. 6. Computed bright field schlieren for rectangular transducer at various sound levels. (a) $v = 2.5$. (b) $v = 5.0$. (c) $v = 7.5$. (d) $v = 10.0$.

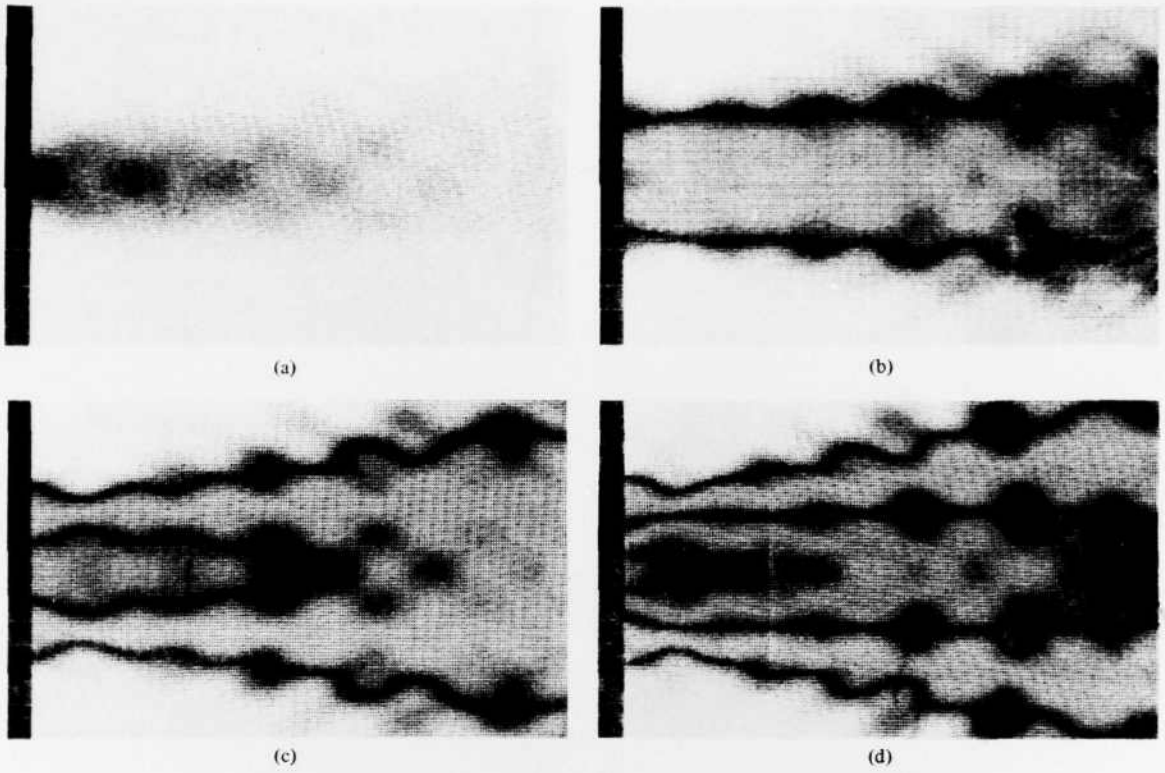

Fig. 7. Computed bright field schlieren for square transducer on its diagonal. (a) $v = 2.5$. (b) $v = 5.0$. (c) $v = 7.5$. (d) $v = 10.0$.

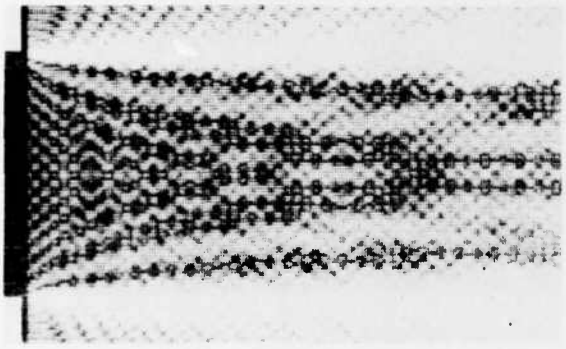

Fig. 8. Computed dark field schlieren approximating the conditions of Fig. 1 of a square transducer with $ka = 45.2$.

tween the gray levels and the field value of v in Fig. 3. However, at higher sound levels, the nonlinear properties of (13) tends to make the patterns more complicated and less interpretable. However, the spreading nature of the sound beam becomes more evident at the higher levels.

An increase of ka also changes the pattern. From the description of Osterhammel's experimental arrangement and an estimation of the sound level, we have computed the image shown in Fig. 8 which is to be compared with Fig. 1. As one can see, many of the geometrical features are duplicated in the calculated image. In fact, the computed image contains some gray areas which are in the original photographs but have been lost in subsequent photographic reproductions. For the pattern shown in Fig. 8, we have chosen a spatial filter that passes only the first diffraction orders. Consequently, intensity assigned to each point is the square of the first-order Bessel function with the argument v. Other schlieren patterns are shown elsewhere [11].

Conclusion

From first principles it is possible to calculate the integrated optical effect for any given transducer configuration in the Raman-Nath region. The numerical technique results from application for Fourier projection slice theorem and does not require explicit integration. Implementation via FFT permits rapid calculations of the integrated optical effect and schlieren patterns.

This procedure can be adapted easily to other configurations such as focused transducers, imperfect transducers, zone plates, and shaded transducers.

Acknowledgment

The authors wish to thank Dr. George Batten, University of Houston, for his assistance with the computer graphic techniques.

References

[1] K. Osterhammel, "Optische Untersuchung des Schallfeldes Kolbenformig Schwinger Quarze," *Akust. Z. Bd.* 6, pp. 73–86, 1941.

[2] W. R. Klein and B. D. Cook, "Unified approach to ultrasonic

light diffraction," *IEEE Trans. Sonics Ultrason.*, vol. SU-14, pp. 123–134, 1967.

[3] F. Ingenito and B. D. Cook, "Theoretical investigation of the integrated optical effect produced by sound fields radiated from plane piston transducer," *J. Acoust. Soc. Am.*, vol. 45, pp. 572–577, 1969.

[4] W. T. Maloney, G. Meltz, and R. L. Gravel, "Optical probing of the Frensel and Fraunhofer regions of a rectangular acoustic transducer," *IEEE Trans. Sonics Ultrason.*, vol. SU-15, pp. 167–172, 1968.

[5] A. J. Crandal, "Measurement of the velocity of sound in water by optical methods," Ph.D. thesis, Department of Physics, Michigan State University, East Lansing, University Microfilms No. 68–7882.

[6] M. E. Haran, B. D. Cook, and H. F. Stewart, "Comparison of an acoustooptic and a radiation force method of measuring ultrasonic power," *J. Acoust. Soc. Am.*, vol. 57, pp. 1436–1440, 1975.

[7] R. Riebold, W. Molkenstruck, and K. M. Swamy, "Experimental study of the integrated optical effect of ultrasonic fields," *Acustica*, vol. 43, pp. 253–259, 1979.

[8] R. Riebold, "The measurement of ultrasonic power using an acousto-optic method," *Acustica*, vol. 36, pp. 214–220, 1976/1977.

[9] J. C. Berlinghieri and B. D. Cook, "Data requirements for mapping of ultrasonic fields with conventional light diffraction," *J. Acoust. Soc. Am.*, vol. 58, pp. 823–827, 1975.

[10] B. D. Cook and F. Ingenito, "Ultrasonic transducer configuration for producing a phase grating of nearly uniform strength," *Proc. IEEE*, vol. 56, pp. 871–872, 1968.

[11] B. D. Cook, "A procedure for calculating the integrated acousto-optic (Raman–Nath) parameter for the entire sound field," presented at the 1979 Ultrasonic Symp., New Orleans, LA, Sept. 26–28, 1979, paper p-8.

[12] E. Meyer and E. Newman, *Physical and Applied Acoustics: An Introduction*. New York and London: Academic, 1972, p. 175.

A PROCEDURE FOR CALCULATING THE INTEGRATED ACOUSTO-OPTIC (RAMAN-NATH) PARAMETER FOR THE ENTIRE SOUND FIELD

B

BILL D. COOK

Cullen College of Engineering
University of Houston Central Campus, Houston, Texas 77004

ABSTRACT

An important parameter in acousto-optics is the so-called Raman-Nath parameter which measures the integrated change of optical path produced by an ultrasonic field. A straight-forward procedure has been developed for calculating this parameter for the entire sound field for an arbitrary velocity profile and arbitrary configuration of a baffled planer transducer. Examples will be shown for the square transducer. The technique is limited to linear acoustics and the Raman-Nath region of acousto-optics interaction.

Figure 1 shows the basic optical arrangement for visualizing ultrasonic fields. The type of spatial filtering performed in plane P_3 dictates the type of pattern seen in the image plane P_4. Most common types of filter choices are the following:

1. Pass only the zeroth order
2. Block only the zeroth order
3. Pass only the first diffraction order

However, the complexity seen in the Schleiren pattern depends on the soundfield and the integration of the optical effect through this field. Figure 2 shows the complexity that can occur in the photograph. In this case, the transducer is rectangular and supposedly moving as a piston. In this paper, we demonstrate that these patterns can be theoretically predicted by modeling the configuration and movement of transducer, the optical integration over the resultant sound field and the spatial filtering. The mathematical details of implementing these calculations are outlined elsewhere[1]. However, it should be noted here that the procedure for calculating the integrated optical effect is rapid as it is implemented by applying the fast fourier transform algorithms and has no integration as given in other techniques[2,3].

Basically, it involves taking the projection of transducer velocity in the direction of light propagation; taking the fourier transform, dividing by the cosine of the angles of plane wave assigned to resultant transform variable[4], accounting for propagation with a phase term and taking the inverse fourier transform. As these are one dimensional transforms, one can calculate the field with close spacing without excess cost.

In the calculations shown, we have applied simple spatial filtering typically done [5]. An arbitrary choice for photographic film response has been included to yield a balance of the gray tones.

Figure 2 is taken from a 1941 paper by Osterhammel[6]. From the parameter given and trial and error estimation of the sound level, we show Figure 3 as an example of the calculation. Many features shown in Osterhammel's photograph are reproduced in our computer results.

A demonstration of the effect of the direction of light propagation to sound field has previously been published[7]. It is duplicated in Figure 4. The light is propagating with respect to the orientation of a square transducer as illustrated. Figure 5 shows the result of calculations with the same orientation but with a different ka.

References

[1]B.D. Cook and E. Cavanagh, submitted to IEEE Trans. Sonics Ultrasonics.

[2]W.F. Maloney, G. Meltz, and R. Gravel, IEEE Trans. Sonics Ultrasonics SU-15, 167-172 (1968).

[3]F. Ingenito and B.D. Cook, J. Acoust. Soc. Am. 45 572-577, (1969).

[4]J.W. Goodman, Introduction to Fourier Optics, (McGraw-Hill, San Francisco 1968) p. 50.

[5]W.L. Moore and J.A. Bucaro, J. Acoust. Soc. Am. 63 60-67, (1978).

[6]K. Osterhammel, Ahust, Z. Bd. 6, 73-86, (1941).

[7]B.D. Cook and F. Ingenito, Proc. IEEE 56 871-872 (1968).

CH1482-9/79/0000-0090$00.75 © 1979 IEEE

Figure 1. left- Optical arrangement for Schleiren.

Figure 2. right- Schleiren photograph with first order passed. Rectangular transducer, ka = 45.

Figure 3. left- Computer generated Schleiren pattern for parameters given in Figure 2.

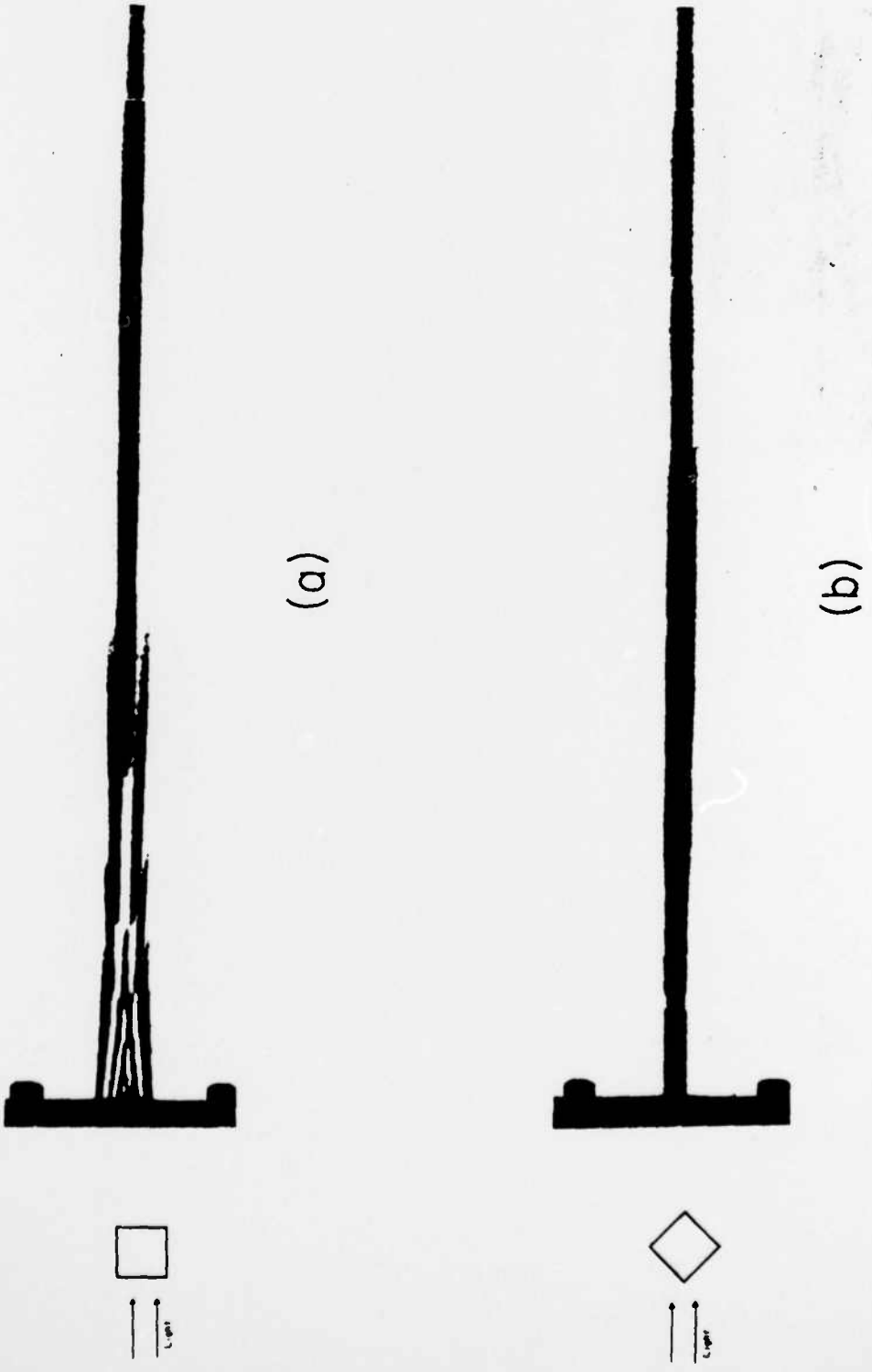

Figure 4. Demonstrated effect of direction of light propagation through the sound field produced by a square transducer.

a.

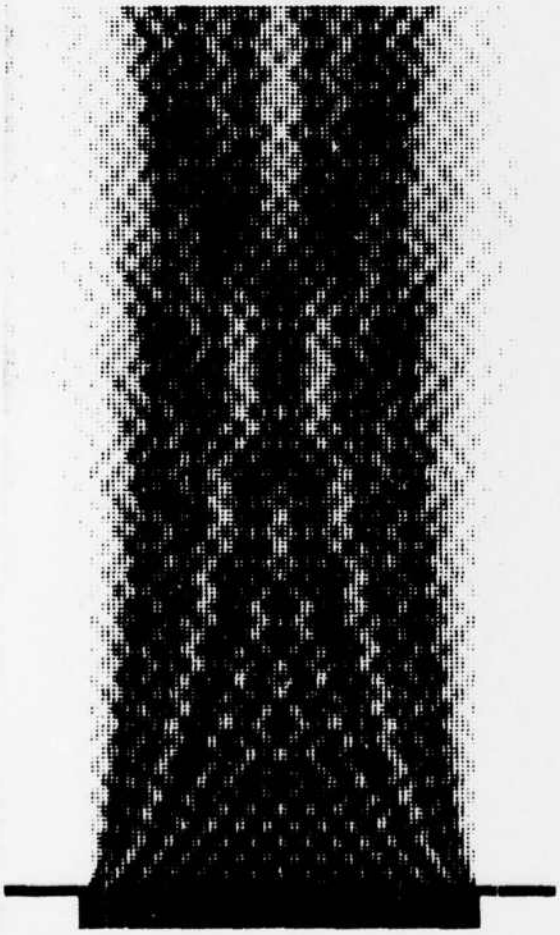

b.

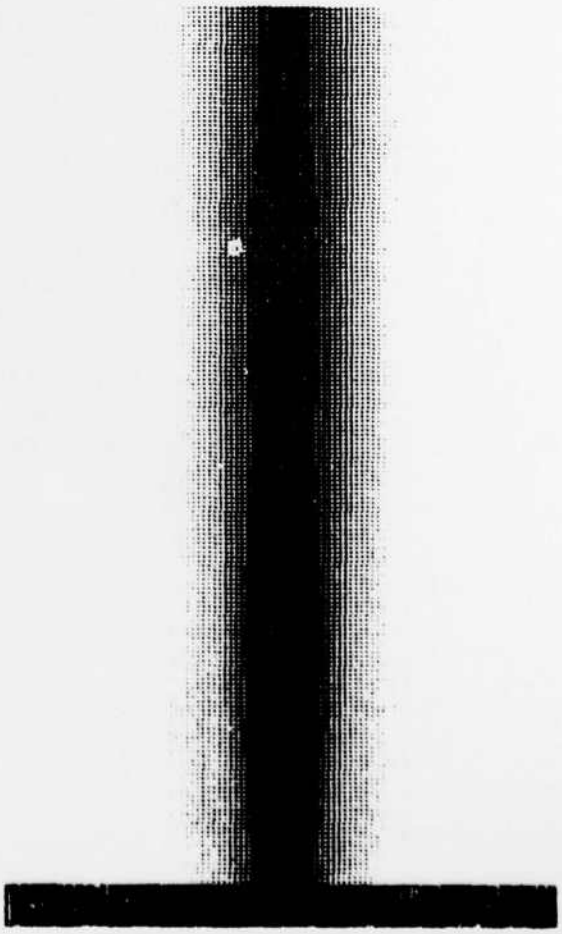

Figure 5. Computer generated Schleiren for parameters of Figure 4, a and b respectively.

Comparison of the experimental and theoretical pressure fields in the nearfield of ultrasonic transducer-lens systems

P. L. Edwards[a)]

The University of West Florida, Pensacola, Florida 32504

Bill D. Cook[a)]

Cullen College of Engineering, University of Houston, Central Campus, Houston, Texas 77004

Henry D. Dardy

U. S. Naval Research Laboratory, Washington, D. C. 20375

(Received 22 April 1980; accepted for publication 23 June 1980)

Experimental measurements of acoustic pressure fields near the focal points of ultrasonic transducer-lens systems are compared to calculations of a recently developed analytic technique. This method incorporates the Fresnel approximation to expand the field in terms of Gaussian-Laguerre functions to calculate the acoustic field for arbitrary placement of a lens in the nearfield of a circular transducer. The predicted field pattern symmetries near the focal region with a lens located either at one focal distance or at the transducer face are confirmed by experimental measurements made with a microsphere probe.

PACS numbers: 43.20.Rz

Recently reported results of Cavanagh and Cook[1,2] establish a method for calculating the acoustic pressure fields in circular ultrasonic transducer–lens systems. Unlike other techniques, this method permits the determination of pressure fields when a lens is placed at an arbitrary position on axis in the nearfield of a circular piston transducer. These calculations indicate that significant spatial field changes occur in the focal region when the position of the lens shifts. In particular, they predict spatial symmetry of the field about the focal plane when the lens is placed one focal length from the transducer; similarly, with the lens located at the surface of the transducer, they predict a pressure maximum shifted towards the transducer rather than at the geometric focal point. This last feature is a known fact of physical optics and has been confirmed experimentally many times.

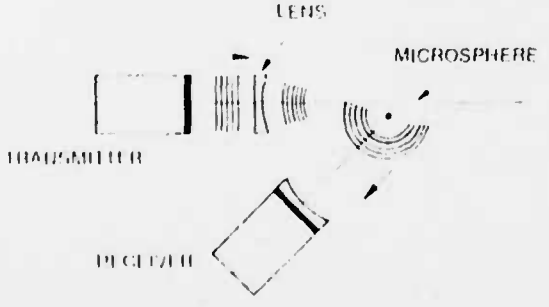

FIG. 1. Experimental apparatus for measurement of pressure field. The microsphere and receiver remain at a fixed position while the source field is processed through their viewing window.

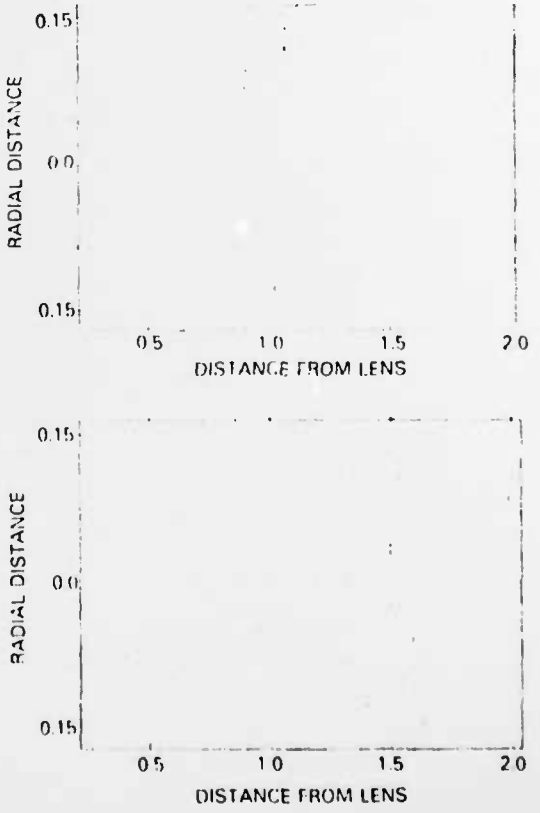

FIG. 2. Calculated pressure field for lens mounted at transducer face (upper) and at one focal distance from the transducer face (lower). Dimensions are in inches.

a)Work performed while at the U.S. Naval Research Laboratory, Washington, D.C., under auspices of Physical Acoustics Center, Code 5130.

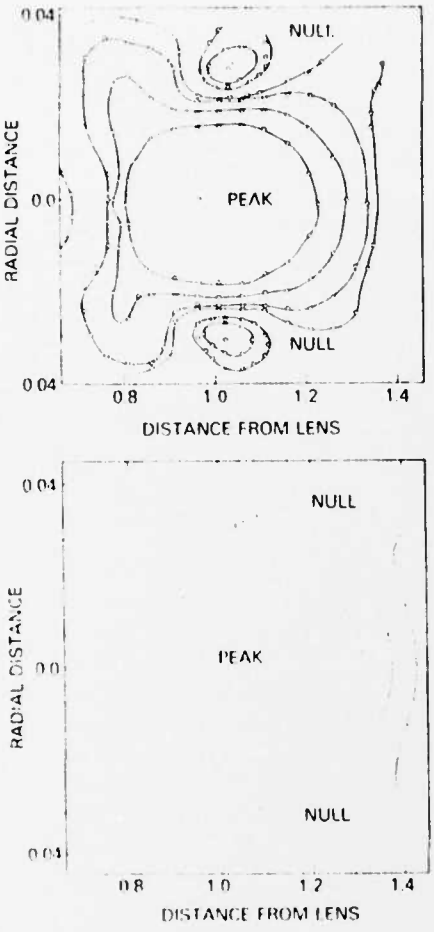

FIG. 3. Experimentally measured (upper) and calculated (lower) pressure contours for lens mounted at transducer face.

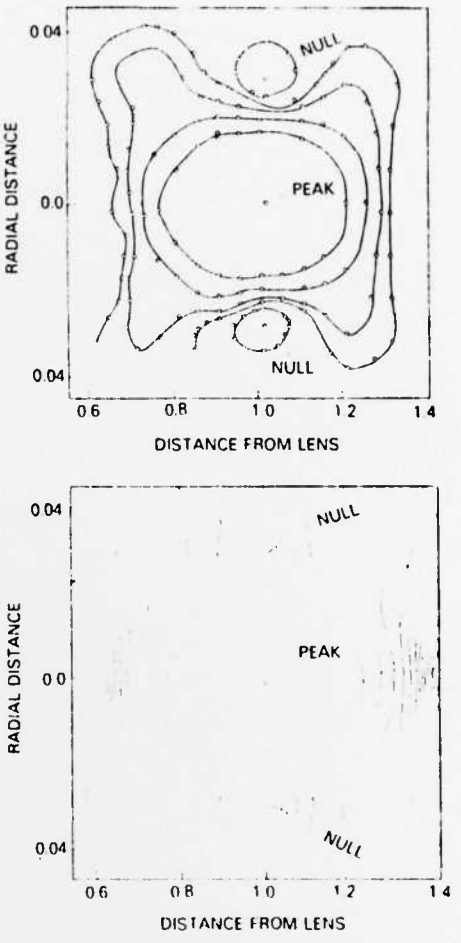

FIG. 4. Experimentally measured (upper) and computed (lower) pressure contours for lens mounted at one focal distance from transducer face.

Experimentally measured values are here compared with calculated values of the field in the region near the focal point for a circular transducer of 0.5 in. diam operating at a frequency of 5.0 MHz. A lucite lens with a focal length of 1 in. was placed coaxially both at the transducer face and at one focal distance from the transducer face. The resulting pressure field was measured by moving a microsphere in rasterlike fashion through the focal region; the technique, developed by Edwards and Lewzynski,[1] utilizes the amplitude of the scattered wave as a measure of the field strength at the microsphere location (Fig. 1). In this arrangement, the microsphere is positioned at the focal point of the receiver and both are held at a fixed position during the course of the experiment. The transmitter and lens system is positioned so that the microsphere interrogates the desired region of the pressure field. The microsphere has a radius of approximately 0.001 in., sufficiently small so that even the focused field presents essentially a uniform field over the area of the sphere. At 5.0 MHz, the product of wavenumber and diameter, ka, is approximately 0.5. The amplitude of the scattered wave is therefore relatively independent of the scattering

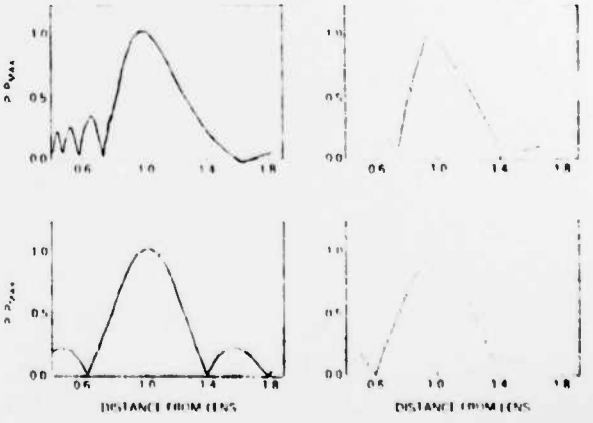

FIG. 5. Comparison of pressure on transducer axis through focal region, computed for lens on transducer face (upper left), measured with lens on face (upper right), computed with lens at one focal distance (lower left), and measured with lens at one focal distance (lower right).

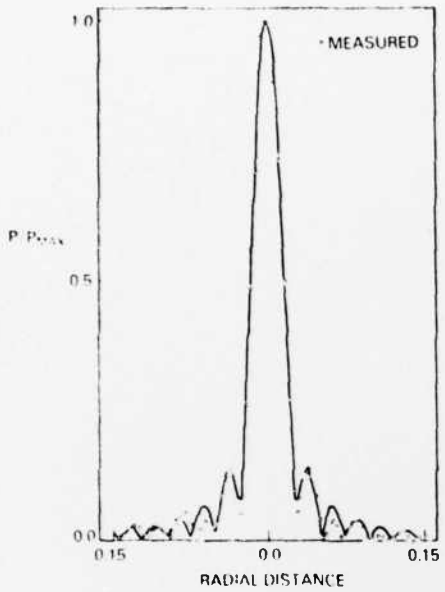

FIG. 6. Measured (•) and computer (-) pressure in the plane perpendicular to the transmitter axis at the point where the axial pressure is a maximum for the case where the lens is mounted on the transducer face.

angles encountered in the experiment.

Figure 2 illustrates the calculated fields for the two transducer-lens geometries. The top diagram illustrates the field obtained for the lens positioned at the transducer face; the same pattern can be expected for the situation of a transducer with a curved radiating surface. The lower diagram, for the lens positioned at one focal length, indicates a significant structural change occurs under these circumstances. In both cases, the abscissa measures the distance from the lens and the ordinate has been expanded to show the resultant spatial detail. Minor differences in the high degree of symmetry exhibited in the lower of the plots is a result of the computer graphic contour routine and not of the analytic development; in both instances the pressure peak in the diagrams is normalized to 0.0 dB and the contours chosen to map 3.0-dB intervals. The experimental and calculated values shown in the remaining figures expand only the central region of these detailed plots.

Measured and computed pressure profiles for the case where the lens is mounted at the transducer face are given in Fig. 3. The measured contour structure in this case is in good agreement with the predicted values; the expanded scale of presentation allows verification of the location of the pressure peaks and nulls. In both diagrams, the contour nearest the peak is −6.0 dB relative to the peak pressure; the remaining intervals are −3.0 dB down (i.e., −9.0 dB, −12.0 dB, etc.). There is an experimental error of approximately 1.0 dB due to the nonlinear response of the measuring electronic equipment.

Figure 4 shows the measured and computed contours for the case where the acoustic lens is placed one focal distance from the transducer face. The measured pressure peak and nulls are again in good agreement with that of the calculation; the measured values verify the high degree of symmetry expected. Calculated and experimental pressure profiles along the transducer axis in the region of the pressure peak are shown in Fig. 5. The upper-left curve shows the calculated pressure for a lens mounted on the source face, the upper right shows the experimentally measured pressure. The lower curves repeat the process for the lens located at the focal distance. The calculated pressure curve in the plane perpendicular to the axis at the point of maximum axial pressure, a distance of approximately 0.96 in. from the lens, is plotted in Fig. 6, along with the experimentally measured values.

Experimental evidence indicates that the method of Cavanagh and Cook adequately predicts the pressure field of ultrasonic transducer–lens system. Calculations, performed point for point with the Gaussian–Laguerre algorithm, allow for quick computation. The results outlined in this work assume the lens large compared to the width of the sound beam. The analytic formulation has been extended to predict the field for finite size lenses. Additionally, the experimental evidence presented indicates the utility of the microsphere probe to spatially map with high resolution and precision the fields encounter in focused ultrasound.

[1] E. Cavanagh and B. D. Cook, "Nearfield of Ultrasonic Transducers–Lens Systems: Theory of the Gaussian–Laguerre Formulation," J. Acoust. Soc. Am. Suppl. 1 66, S40 (1979).
[2] E. Cavanagh and B. D. Cook, "Description of Ultrasonic Fields Using Gaussian–Laguerre Formulation. Numerical Example: Circular Piston," J. Acoust. Soc. Am. 68, 1136–1140 (1980).
[3] P. L. Edwards and J. Arzynski, "Experimental and Theoretical Study of the Scattering of Focused Ultrasound from Microparticles in Fluids," J. Acoust. Soc. Am. Suppl. 1 65, S128 (1979).
[4] P. L. Edwards and J. Arzynski, "Use of a Microsphere Probe for Pressure Field Measurements in the Megahertz Frequency Range," J. Acoust. Soc. Am. 68, 356–358 (1980).


DATE
ILME

FIG. 1. Experimental apparatus for measurement of pressure field. The microphone and receiver remain at a fixed position while the source field is processed through their viewing window.

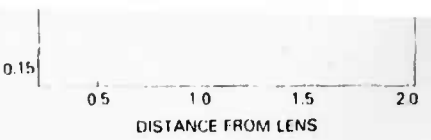

FIG. 2. Calculated pressure field for lens mounted at transducer face (upper) and at one focal distance from the transducer face (lower). Dimensions are in inches.

[1]Work performed while at the U.S. Naval Research Laboratory, Washington, D.C., under auspices of Physical Acoustics Center, Code 5120.

of the experiment. The transmitter and lens system is positioned so that the microsphere interrogates the desired region of the pressure field. The microsphere has a radius of approximately 0.001 in., sufficiently small so that even the focused field presents essentially a uniform field over the area of the sphere. At 5.0 MHz, the product of wavenumber and diameter, ka, is approximately 0.5. The amplitude of the scattered wave is therefore relatively independent of the scattering

FIG. 6. Comparison of pressure on transducer axis through focal region, computed for lens on transducer face (upper left), measured with lens on face (upper right), computed with lens at one focal distance (lower left), and measured with lens at one focal distance (lower right).